

ALE-AMR: A new 3D multi-physics code for modeling laser/target effects

This article has been downloaded from IOPscience. Please scroll down to see the full text article.

2010 J. Phys.: Conf. Ser. 244 032019

(<http://iopscience.iop.org/1742-6596/244/3/032019>)

View [the table of contents for this issue](#), or go to the [journal homepage](#) for more

Download details:

IP Address: 50.136.219.251

The article was downloaded on 18/04/2013 at 01:32

Please note that [terms and conditions apply](#).

ALE-AMR: A New 3D Multi-Physics Code for Modeling Laser/Target Effects

A. E. Koniges¹, N. D. Masters², A. C. Fisher², R. W. Anderson², D. C. Eder², T. B. Kaiser², D. S. Bailey², B. Gunney², P. Wang², B. Brown², K. Fisher², F. Hansen², B. R. Maddox², D. J. Benson³, M. Meyers³, A. Geille⁴

¹Berkeley Lab, USA, ²LLNL, USA, ³UCSD, USA, ⁴CEA, DAM, CESTA, France

Email: aekoniges@lbl.gov

Abstract. We have developed a new 3D multi-physics multi-material code, ALE-AMR, for modeling laser/target effects including debris/shrapnel generation. The code combines Arbitrary Lagrangian Eulerian (ALE) hydrodynamics with Adaptive Mesh Refinement (AMR) to connect the continuum to microstructural regimes. The code is unique in its ability to model hot radiating plasmas and cold fragmenting solids. New numerical techniques were developed for many of the physics packages to work efficiently on a dynamically moving and adapting mesh. A flexible strength/failure framework allows for pluggable material models. Material history arrays are used to store persistent data required by the material models, for instance, the level of accumulated damage or the evolving yield stress in J2 plasticity models. We model ductile metals as well as brittle materials such as Si, Be, and B4C. We use interface reconstruction based on volume fractions of the material components within mixed zones and reconstruct interfaces as needed. This interface reconstruction model is also used for void coalescence and fragmentation. The AMR framework allows for hierarchical material modeling (HMM) with different material models at different levels of refinement. Laser rays are propagated through a virtual composite mesh consisting of the finest resolution representation of the modeled space. A new 2nd order accurate diffusion solver has been implemented for the thermal conduction and radiation transport packages. The code is validated using laser and x-ray driven spall experiments in the US and France. We present an overview of the code and simulation results.

1. Introduction

The extreme range of physical conditions (temperature, density, pressures, etc.) and spatial scales (microns to meters) associated with modeling debris/shrapnel generation at large laser facilities (Omega, NIF, Orion, LMJ, etc.) motivated a new numerical approach to simulations. This approach based on combining Arbitrary Lagrangian Eulerian (ALE) hydrodynamics with Adaptive Mesh Refinement (AMR) provides great flexibility but introduces many algorithmic challenges. The new code, ALE-AMR, builds off the early work in incorporating ALE and AMR for gas-dynamics [1]

using the Structured Adaptive Mesh Refinement Application Interface (SAMRAI) [2]. The addition of multi-material and the corresponding interface reconstruction capability provides the flexibility to relax the need to force material boundaries to correspond to zone boundaries. This allows one to place a complex configuration on a mesh and allow the AMR to add zones to refine the interfaces [3]. The AMR capability is also used dynamically to provide higher resolution in regions with steep gradients during simulations. The implementation of an anisotropic stress tensor and support for numerous strength/failure models provides the flexibility to model a wide range of materials using anything from analytical flow-stress models to detailed single-crystal plasticity models [4]. The code models both ductile metals used for shields, diagnostic filters, etc., as well as brittle materials such as Si, Be, and B4C used for cryogenic cooling/support and diagnostic filters.

The initial deposition of energy is generally by 3ω laser light with 1ω and 2ω laser light being important for some structures. Laser rays at the different frequencies are propagated through a virtual composite mesh consisting of the finest resolution representation of the modeled space with inverse bremsstrahlung absorption [5]. The energy deposited by the laser can create hot plasmas with subsequent energy transfer occurring by thermal conduction or radiation. A new 2nd order accurate diffusion solver has been implemented for the thermal conduction and radiation transport packages [6]. As an example of the current capability, we can model a target component heated by a laser that becomes a hot plasma with the resulting radiation striking another component producing ablation and the launch of a shock through the component. This shock can reflect at a free boundary and produce a tensile wave and subsequent spall. The code can calculate the spall including size of spall fragments and velocities. This information is used to determine if optics or diagnostics are at risk. If the shock or radiation causes the spall material to be molten, a surface tension model is required to predict droplet sizes of spall material. We are currently studying different surface tension models with collaborators at UCLA to determine which models are appropriate for the ALE-AMR code.

2. Overview of the ALE-AMR code

The code is based on Lagrangian hydrodynamics with position and velocity being nodal variables and density, internal energy, temperature, pressure, strain, and stress being zonal (cell centered) variables. (The thermal conduction and radiation transport equations are solved using the diffusion approximation with temperature and radiation energy being additional nodal variables.) The hydrodynamic equations are:

$\frac{\partial \rho}{\partial t} + \nabla \cdot (\rho \vec{v}) = 0$	Continuity Equation
$\rho \frac{\partial \vec{v}}{\partial t} = \nabla p + \nabla \cdot \Sigma' + \rho \vec{b}$	Momentum Equation (with deviatoric stress tensor shown)
$\rho \frac{\partial e}{\partial t} + p \nabla \cdot \vec{v} = 0$	Energy Equation
$\Sigma^{n+1} = f(\Sigma^n, \rho, e, \vec{v}, p, T, \vec{h})$	Material Stress Update

The equations are closed through the use of the equation of state (EOS), which is often tabulated. The EOS specifies the thermodynamic relation between state variables, such as internal energy, density (volume), pressure and temperature. Cells can have multiple materials with the volume fraction of each material in a mixed cell being tracked. If needed, e.g., for mesh refinement, interfaces are constructed using the volume fractions of neighboring cells. In mixed cells, the zonal hydrodynamic variables are determined for each material but averaged quantities are calculated and used for the hydrodynamic step. If the mesh becomes unacceptably distorted, the mesh is relaxed and all variables are mapped/advection to the new mesh. The different physics packages are included in an operator splitting approach. Parallel domain decomposition and the corresponding message passing is primarily treated within SAMRAI allowing the code to run efficiently on parallel computing architectures.

3. Code Validation

The code is also being validated with microscopic laser and x-ray induced spall experiments in the US and France. Figure 1 and 2 show results of a laser-induced spall experiment. The properties of the spall material, i.e., size, number, and velocity of fragments, obtained from ALE-AMR simulations are compared to observed data from in-flight images and aerogel samples. Similar experiments have been conducted in France using x-rays from a laser heat Au foil to induce spall in a range of different foils.

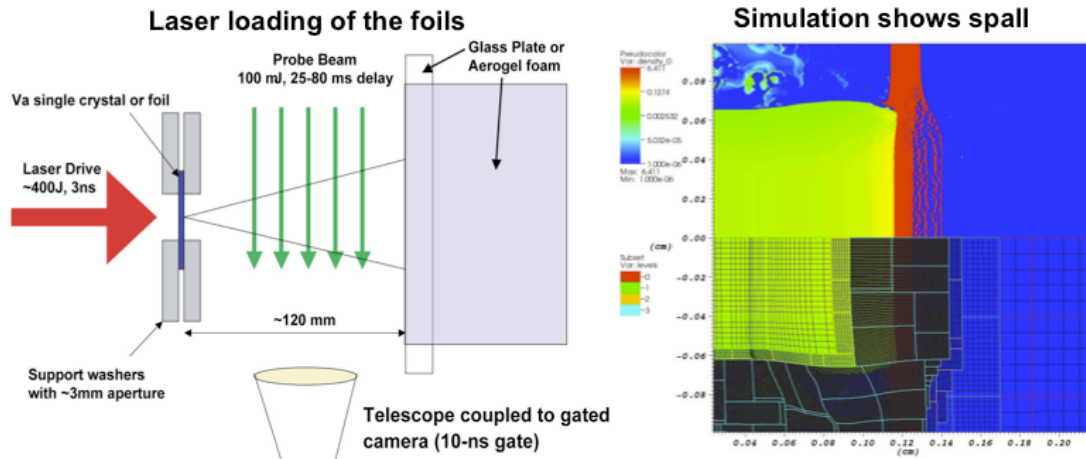


Figure 1 Laser induced spall experiment at LLNL with fragment capture and imaging. ALE-AMR simulation on right with mesh refinement shown in lower half.

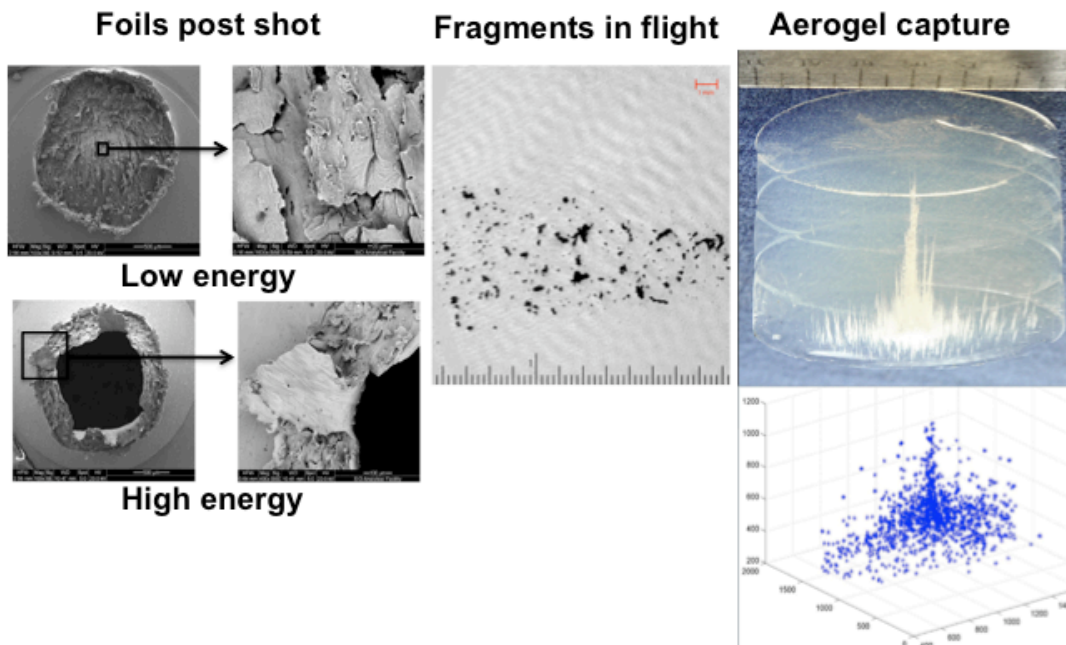


Figure 2 Foils for low-laser energy show spall while high energies leave hole in foil. Fragments observed in flight. Capture in aerogel with size and depth of fragments used to calculate velocity.

4. NIF Simulations

A schematic of the NIF chamber is shown in Figure 3. A cryogenic target is inserted from the right and the 3D simulation on the right is for a cryogenic cooling ring. Coming in from the left side is a diagnostic snout used for x-ray imaging. A close up of the snout is given in Figure 4. Inside the snout

is a pinhole array with front and rear collimators. We show results of ALE-AMR simulations on a single pinhole for 3 levels of x-ray loading. A wide range of NIF experiments have been modeled.

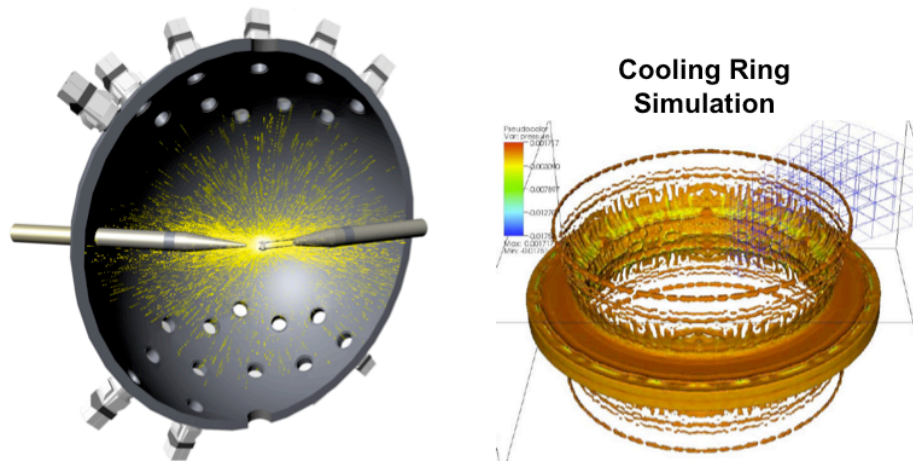


Figure 3 NIF chamber with target and diagnostic inserted. ALE-AMR simulation on right.

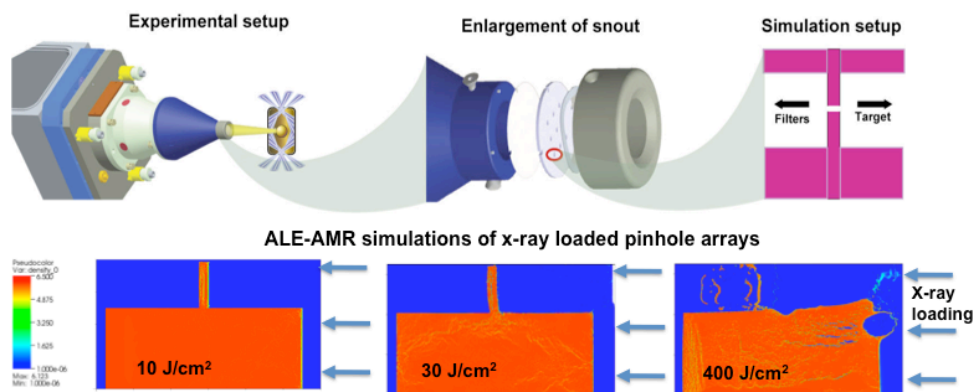


Figure 4 Diagnostic snout with pinhole array modeled by ALE-AMR.

5. Conclusion

The ALE-AMR code is being used to design experiments at large laser facilities through out the world. Its unique capabilities are being used to mitigate the impact of debris/shrapnel generation. New numerical techniques were developed for many of the physics packages to work efficiency on a dynamically moving and adapting mesh. The code is also being applied to new areas including warm-dense-matter experiments at LBL and slurry flow experiments at UCLA.

References

- [1] Anderson R W, Elliott N S and Pember R B 2004 *Journal of Computational Physics* **199** 598
- [2] Wissink A M, Hornung R D, Kohn S R, Smith S S and Elliott N S 2001 *SC01 Proceedings* (Denver, CO) Also available as LLNL technical report UCRL-JC-144755.
- [3] Masters N, Anderson R, Elliott N, Fisher A, Gunney B and Koniges A 2008 *Journal of Physics: Conference Series* **112** 022017
- [4] Fisher A C, Masters N D, Dixit P, Benson D J, Koniges A E, Anderson R W, Gunney B T N, Wang P and Becker R 2008 *Journal of Physics: Conference Series* **112** 022027
- [5] Masters N D, Kaiser T B, Anderson R W, Eder D C, Fisher A C, and Koniges A E, *in this series*
- [6] Fisher A C, Bailey D S, Kaiser T B, Gunney B T N, Masters N D, Koniges A E, Eder D C, and Anderson R W *in this series*